Contents lists available at ScienceDirect

Displays

journal homepage: www.elsevier.com/locate/displa

Effects of speed, complexity and stereoscopic VR cues on cybersickness examined via EEG and self-reported measures

Alper Ozkan[a], Ufuk Uyan[a], Ufuk Celikcan[a,*]

[a]*Hacettepe University, Department of Computer Engineering, Ankara, 06800, Turkey*

ARTICLE INFO

Communicated by

Keywords:
Virtual Reality
Cybersickness
EEG
Head Mounted Displays

ABSTRACT

This study evaluated the interplay between environmental cues in virtual reality (VR) and cybersickness as experienced by users of head-mounted displays (HMDs). Utilizing electroencephalogram (EEG) data and self-reported discomfort measures, the effects of three major VR cues - speed, scene complexity, and stereoscopic rendering - on cybersickness were examined, with the latter being of particular interest as it had not previously been studied explicitly in the context of VR-HMDs. Self-reported discomfort was assessed through in-VR single-item queries and post-VR simulator sickness questionnaires, accounting for both immediate and persistent cybersickness, respectively, and over three experiment sessions, accounting for the effects of accumulation. Analysis revealed connections that indicate a relationship between EEG data and the presence of cybersickness for all three cue types. Significant differences were observed in EEG relative power changes between the trials where cybersickness was and was not reported. EEG relative power changes were also linked to both immediate and persistent cybersickness, especially in the theta and gamma frequency bands. The increase in immediate discomfort with the stereoscopic rendering cues over successive sessions suggests a decrease in tolerance to these effects over time.

1. Introduction

Despite the tremendous progress achieved in virtual reality (VR) technologies, cybersickness remains a central issue in VR [1]. It has been revealed that modern VR head-mounted displays (HMDs), with their increased level of immersion, can lead to more severe instances of cybersickness compared to less immersive VR setups [2].

Cybersickness, which presents during or following exposure to virtual environments (VEs) [3], is akin to motion sickness and commonly manifests as headaches, eye strain, nausea, and dizziness [4]. However, cybersickness can be triggered purely by visual stimuli in the absence of actual movement. Theoretical evidence suggests that conflicts between visual and vestibular stimuli are the main cause of cybersickness. This is supported by the observation that more realistic-looking VEs can induce more intense symptoms [5] as the enhanced visual stimuli provide the user with more information about the environment, making it harder to dismiss the conflict. Cybersickness can reduce user comfort severely and hinder access to VR applications that serve therapeutic, rehabilitative, or educational purposes [6]. While there are practices that can alleviate cybersickness within VEs, such as reducing the field of view [7] or using background images [8], they can be detrimental to user experience when utilized constantly, and should therefore be applied only when cybersickness occurs, or, better yet, is anticipated.

In VR, another primary issue is the vergence-accommodation

*Corresponding author: E-mail:ufuk.celikcan@gmail.com; Tel.: +90-312-297-7500;

http://dx.doi.org/10.1016/j.displa.xxxx.xx.xxx
Received ; Received in final form ; Accepted ; Available online
0141-9382/

conflict (VAC), which can be exacerbated with systems using stereoscopic vision to convey an enhanced sense of depth [9]. With VAC, discomfort arises because of the mismatch between vergence, where the eyes meet as the object of interest, and accommodation, where the eye lenses are tuned to focus on. In natural viewing, there is usually no conflict as vergence matches accommodation. On the contrary, when viewing VEs via stereoscopic vision, the object of interest can be rendered behind or in front of the display, resulting in vergence being directed towards the object while accommodation remains on the display. The conflicting cues lead to a feedback loop that provokes discomfort. Although human visual system have some degree of tolerance towards VAC, the effect becomes tiring with long term use, especially with extended severe mismatch [10], and contributes to cybersickness [11, 12].

With this work, we investigate the effects of three major VR cues - speed, scene complexity, and stereoscopic rendering parameters - that factor into cybersickness via sensory conflicts [4]. To evaluate the effects of simulating these cues in varying degrees, we make use of participants' self-reported measures of cybersickness as well as their brain activity. The simulator sickness questionnaire (SSQ) [13], consisting of nausea, oculomotor, and disorientation subscales in a total of 16 items, has been the most frequently applied self-reported measure in cybersickness research. However, its use has been subject to criticism due to its breadth as the the discomfort may considerably diminish during the time spent administering the questionnaire [14]. For that reason, there have been studies [15, 16] that have used single-question inquiries of discomfort for immediate self-assessment. In this work, we adopted a combination of SSQ and a single-question inquiry together for a comprehensive assessment of cybersickness that covers both immediate and long-term VR-induced discomfort, thus enabling a comparison between the two.

As an objective and more direct response to cybersickness, it is possible to make use of biofeedback such as electroencephalogram (EEG), electrocardiogram (ECG), blood pressure, electrogastrogram (EGG), respiration, and skin temperature to estimate the severity of cybersickness related symptoms. In this study, EEG signals measured via a wireless mobile headset (Emotiv Epoc+) have been used for the headset provides ease of application together with ample biofeedback direct from the regions of the brain associated with cybersickness [17]. EEG signals comprise of waves that manifest in different shapes, frequencies and amplitudes according to the subject's physiological and psychological state. They provide rich timely biofeedback with multiple spatial components by different electrodes. Accordingly, EEG data has been shown to be beneficial in the study of brain activity arising with neuron interaction [18] and bears significant potential for use in cybersickness detection and mitigation [19].

Overall, our aim has been to broaden the insight into cybersickness by comprehensively examining the effects of speed, scene complexity and stereoscopic rendering on cybersickness experienced with VR-HMDs. By exposure to these cues at varying levels, we evaluated subjects' responses through measures of brain activity and two types of cybersickness reports, one probing in-VR immediate discomfort with a single-item query and the other probing post-VR persistent discomfort with SSQ. Additionally, we considered personal factors including susceptibility to motion sickness, level of VR experience and video gaming frequency. For this evaluation, the subjects were immersed in a VE that had been uniquely designed to induce cybersickness by varying the severity of each cue through a set of predefined levels in isolation (using separate scenes implemented in the same VE) while simultaneously acquiring their brain activity response using EEG. The collected data were analyzed in relation to the cue types and their severity levels as well as time spent in VR, accounting for the effects of accumulation.

2. Previous Work

Cybersickness has been widely researched following the Kolasinski's work in 1995 [20], which cited multiple factors including frame rate and tracking errors as its probable causes. Several recent studies [21, 22, 11] offered extensive overviews laying out many other factors focused on by a large body of work.

Visually simulated movement speed has been one of the most widely studied factors of cybersickness [23, 24, 25]. Movement is an important aspect of an immersive virtual experience as a user's ability to move around the VE reinforces the spatial aspect of the environment and allows for richer interactions. However, short of certain exceptions such as teleportation, most VR locomotion methods invoke vection, *i.e.* illusory self-motion. This perceived movement in the absence of real physical movement is not felt by the vestibular system, causing further discomfort with increasing speed. So et al. [26] reported that movement speed had a significant effect on the oculomotor discomfort subscore of SSQ, which is related to symptoms concerning vision. In another work [27], they also showed that nausea and total sickness severity increase linearly with speed. Keshavarz et al. [24] reported the intensity of vection and its duration are connected to the speed. This is supported by the theory that sensory conflict, a major cause of cybersickness [4], intensifies as speed increases. Further, earlier studies exhibited that the mismatch between perceived and physical head movements significantly contributed to symptoms of cybersickness [28, 29]. It was also shown that introducing consistent stereoscopic depth cues augmented linear vection along different trajectories [30, 31].

Some studies employed virtual roller coasters as they allow for winding paths with many turns and high speed to induce vection and cybersickness. Wibirama et al. [23] inspected the effects of fixation points on cybersickness with roller coasters. They found higher speed and real world footage of roller coasters induced more intense cybersickness than slower and computer generated ones, respectively. Nalivaiko et al. [32] investigated the effects of cybersickness on the cardiovascular system using biometrics and found the more realistic "Helix" simulation induced more nausea in users. Krokos et al. [33] used a set path of motion, with a design similar to a virtual roller coaster, taking place in outer space and allowed participants to report

occurrence of cybersickness in real time with a joystick. They reported increases in brain activity aligned with presence of cybersickness in their time-frequency analysis.

Scene complexity, also referred to as spatial complexity or scene density [34, 35], has been identified as another significant factor in the onset of cybersickness [4]. While limited studies have explicitly examined the effects of scene complexity on cybersickness, a growing body of literature that focused on different aspects of it suggests that it can be defined as a composite metric with multiple elements, including the number of objects, color variety, movement patterns, and associated particle effects present in a VE. Kavakli et al. [36] posited the notion that as scene complexity increases, so too does the incidence of cybersickness, in parallel with the amount of visual complexity and motion information present. Liu et al. [5] suggested that the increase in the symptoms of cybersickness with elevated scene complexity might be due to the increasing amount of depth cues and the sense of presence, making the sensory conflict more intense. Keshavarz et al. [24] found that the intensity of vection is directly impacted by the crowdedness of a scene. Terenzi et al. [37] studied reactions of users to varying particle fields with different acceleration and optic flow types. They reported that different thresholds of discomfort related to different flow fields.

Effects of cybersickness have been studied on different types of biometric feedback. Cebeci et al. [38] examined eye-related feedback along with heart rate change while users were shown VEs that are designed to invoke different emotional responses and observed a significant effect of the scene context on saccade mean speed, saccade rate, pupil dilation, fixation count, fixation duration, and heart rate. Naqvi et al. [39] reported significantly higher SSQ ratings and significantly lower low frequency to high frequency ratio in the ECG signals in users exposed to 3D stimulus than 2D. Dennison et al. [40] used a variety of biometric responses including EGG, heart rate and electrooculogram (EOG) and reported a significant relationship with the SSQ scores.

Kim et al. [41] investigated the effects of cybersickness and time spent in the VE and found significant correlations between the time spent, SSQ scores and certain EEG relative band powers, heart rate, eye blink rate, skin conductance, gastric tachyarrhythmia and respiration rate. Especially with regard to EEG, their findings indicate a significant connection between beta and delta frequency band powers and cybersickness. They also suggested that cybersickness activity observed in EEG is likely a variant of seizure activity as it exhibits analogous behaviour. Similarly, Chang et al. [8] pointed out the presence of attenuated alpha and beta waves when their users are subjected to heavier cybersickness inducing stimuli. Another study indicated correlation of the theta band power with increasing cybersickness [42]. Chen et al. [43] investigated the effect of motion sickness on EEG signals with a car simulator on a winding tunnel and found connections including spectral changes in parietal and occipital areas. Jang et al. [44] compared the cybersickness EEG responses of user groups with low and high motion sickness susceptibility in VR. The high susceptibility group reported higher scores of SSQ and lower absolute bandpowers for the beta and gamma frequency bands. Oh et al. [34] used a collection of 52 VEs with different parameters such as background, movement speed and field of view and collected EEG, ECG and galvanic skin response. They highlighted increasing delta frequency band power and decreasing beta and gamma frequency band powers with higher reports of cybersickness. Nurnberger et al. [45] included horizontal and vertical directions of motion and speed and found increasing levels of discomfort with higher speed and increasing variety of motion, which were also identified with increased activity from lower frequency bands (delta, theta and alpha) in the EEG recordings.

Researchers studied visual conflicts in relation to the discomfort felt with various types of stereoscopic displays [46, 47, 48, 49] including VR-HMDs [50, 51]. Szpak et al. [10] compared two groups, in one of which participants were immersed in a VE, and reported that the VE group exhibited significant differences in sight and accommodation abilities. Kim et al. [52] studied the intensity of visual fatigue invoked by 2D and 3D displays and its effects on EEG signals. They reported significantly higher visual discomfort with 3D content and significantly higher average power of beta frequency observed in EEG. Zou et al. [53] looked into certain ratio indices such as θ/α and θ/β. They found significant differences for the alpha and beta rhythms and multiple ratio indices involving alpha band power for pre-VAC and post-VAC measurements along with electrode location differences for all observed signals. Zheng et al. [54] reported EEG band power correlations with VAC, mainly in the alpha and delta bands and the ratio indices used in the former study [53]. Yildirim [55] investigated display type effect on players' cybersickness and enjoyment. He found that although HMDs induce significantly more discomfort compared to flat displays while gaming, they do not provide a significant increase in enjoyment. He then extended this study by evaluating the feeling of sickness across two different games, a car racing game and a first person shooter [56]. Significant differences were found in the severity of cybersickness felt with HMDs than playing on a regular screen in both cases. Somrak et al. [57] compared the use of various HMDs and a 2D TV for reference and obtained similar results, that is, all HMDs that they tested inflicted more discomfort than the 2D TV. Wibirama et al. [58] investigated the effect of both user activity (whether they were players or spectators) and movement type in game (optical flow like movement in racing games and arbitrary movement in shooter games) on cybersickness in stereo 3D contents. They found that being a spectator and the content with unpredictable movement increased the rating of discomfort.

In this work, instead of focusing on a single control variable, we evaluate the effects of three major VR cues, namely speed, scene complexity and stereoscopic rendering parameters, on cybersickness. There seem to be only a few studies that have extensively addressed the effects of scene complexity. Also, to our knowledge, no other work has investigated the effects of different stereoscopic rendering parameters on cybersickness experienced with immersive VR-HMDs. Contrarily, we investigate the effects of varying these cues on cybersickness in parallel within the same controlled VE that is viewed on a commonly

available VR-HMD. Moreover, we carried our evaluation of invoked cybersickness as reflected by the simultaneously collected EEG feedback and corresponding self-reported measures of VR discomfort. Since the three cues under consideration here are all content-related factors (i.e. factors that can be controlled using software), it is possible to alter them automatically on the fly. Hence, an extensive analysis that presents the effects of varying these cues on EEG response conjointly is to provide valuable insight for future work, notably for designing methods of mitigating cybersickness via adjusting one or more of these cues based on timely brain activity feedback.

3. Materials and Methods

We have administered a within-subject user study by means of a VE with cybersickness inducing content via three different types of VR cues. The study had been approved by the ethics board at Hacettepe University. The components of the user study are discussed in the following subsections.

3.1. Participants

To gather participants for the study, a campus-wide announcement was made at Hacettepe University. Participants responded to volunteer by filling out an online form.

All participants validated that they did not suffer from epilepsy. They were also tested to make sure they can observe stereoscopic depth, have normal or corrected to normal vision acuity while viewing the VE with the HMD and are not color blind.

Initially, 40 people who passed the screening were admitted to the study. However, five of them could not complete all three sessions due to schedule conflicts. From the remaining group, two of them reported not having felt any discomfort throughout the experiment so the data from these participants were discarded in the analysis. Thus, our final sample consisted of 33 people (7 females, 26 males) aged 18-42 (mean age 23.8±5.56). The participants had an average MSSQ percentile of 29.7±22.7 (out of 100), indicating low average susceptibility in the sample. Their overall level of experience with VR was also low (0.9±1.1 mean on a 0-4 scale) and they had moderate video gaming habits (2.1±1.4 mean on a 0-4 scale).

3.2. Experimental Procedure and the Virtual Environment

During the experiment, participants experienced the VE in three repeating sessions. In each session, they went through three scenes, each corresponding to a different cue (movement speed, stereoscopic rendering or scene complexity) at varying stimulus levels. The overview of the experimental procedure is illustrated in Figure 1, which includes sample frames of each scene. The scenes are detailed in the following subsections. The complete scenes can be viewed in the supplementary video material.

The VE was designed and rendered using Unity graphics development engine and SteamVR. It was viewed with an HTC Vive VR system running at 1080x1200px resolution per eye.

Prior to the experiment, participants were fully informed of the experimental procedure, possible side effects of VR, and cybersickness, as well as their right to terminate the experiment at any time. They were instructed to refrain from speaking during the experiment, except during breaks between levels or if they need to end the experiment immediately. Participants provided written informed consent to participate in the study, and completed a demographic questionnaire, in which they indicated their video gaming frequency and level of VR experience in addition to demographic information anonymously. They also filled out a motion sickness susceptibility questionnaire (MSSQ).

Interpupillary distance of each participant was measured using a digital pupillometer and the separation of the HMD lenses was adjusted accordingly. Participants were fitted with an EEG headset, HTC Vive (HMD), and hand controller, and underwent a tutorial session until they felt comfortable and proficient with the VE.

When participants declared their proficiency with the system, the tutorial was ended, and a baseline EEG response was acquired by showing the test environment with default lighting and no motion or external stimuli for 10 seconds. Participants then completed their first SSQ and proceeded to the experimental phase.

In the experiment, each scene simulated a separate cue and consisted of a series of levels, where the simulated cue varied according to a predefined set. During a level, participants were instructed to watch a focus object, a blue octahedron with a glowing effect, while it moved down a wide dark corridor on a winding path for 10 seconds. The camera tracked the focus object from a close distance. As it moved, the focus object oscillated horizontally, requiring participants to shift their gaze between left and right.

Following the simulation of each level, participants were asked to rate the amount of discomfort felt during that level on a scale of 1 (“none at all”) to 7 (“extremely”), henceforth referred to as *immediate discomfort score* (IDS). Participants

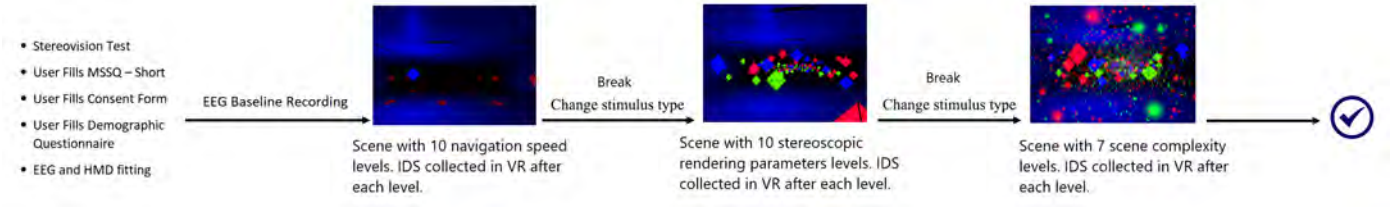

Figure 1: Flowchart of the experimental procedure for a single session. Each participant experienced three such sessions, in which the scenes were ordered in a 3x3 Latin square design.

were instructed to assign a score of 1 to indicate the absence of discomfort and to use a score of 2 or higher to indicate any discomfort experienced, with the score reflecting the perceived severity of the discomfort. After registering the IDS, the application proceeded to the next level according to the predefined order for the simulated cue set when participants pressed the designated hand controller button indicating readiness to continue.

Once all levels of the simulated cue were completed, a black screen was displayed for a minimum of 30 seconds to allow participants rest their eyes and recollect themselves. Then, the scene for the next cue was initiated when the participant expressed readiness to continue by pressing the designated hand controller button.

When all three scenes were shown, a session was concluded and participants were asked to remove the HMD and fill out another SSQ. In a single session, a total of 270 seconds of EEG data was collected per participant and approximately 9-10 minutes were spent in VR, including baseline recordings and breaks between levels.

After resting their eyes for a minimum of three minutes following the end of a session, participants were asked if they were able to continue the experiment and reminded of their right to terminate the experiment at any time. Upon their approval, they were refitted with the HMD and immersed in the VE for another session.

The experiment concluded when participants were exposed to the VE for three such sessions, in which the cue scenes were presented in a randomized order with a 3x3 Latin square design to offset carry-over influences between different cues.

3.2.1. Movement Speed

In the movement speed trials, a set of ten levels of movement speed was simulated (1.2, 2.4, 4.8, 9.6, 14.4, 19.2, 28.8, 38.4, 57.6, and 76.8 meters/sec for the consecutive levels) as illustrated in Figure 2. During the simulation, speed of the focus object was set to the corresponding movement speed (i.e., the speed of the scene camera acting as the participant's viewpoint in the VE) in each level. The scene contained bright red arrows placed on the surrounding walls and the floor in addition to the focus object to promote the sense of vection. An emission shader was applied to the arrows that made them unaffected by the scene lighting, thus allowing them to be seen independently from the focus object as it was otherwise the only light source in the environment.

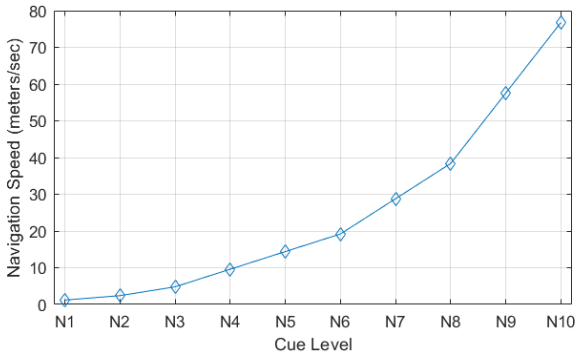

Figure 2: Plot showing movement speed values for each cue level.

3.2.2. Stereoscopic Rendering Parameters

To study the influence of different stereoscopic rendering settings, we utilized the two principal stereoscopic camera parameters: interaxial-distance, the distance between the two cameras rendering the scene for each eye, and zero-parallax distance, where the image for the left/right cameras are identical. By altering these two parameters via projection manipulations [59] from the values that are fixed by default in commercial VR-HMDs (Table 1), we evaluated the effects of stereoscopic imagery with a variety of disparity settings.

Ten different pairs of interaxial-distance and zero-parallax distance (Table 1) were tried in this scene as illustrated in Figure 3. Only one of the two parameters was changed between consecutive stimulus levels. Initially, the scene was rendered using a moderate interaxial-distance and relatively low zero-parallax distance setting. The zero-parallax distance was then linearly increased until the fourth level. After this, the interaxial-distance was increased in the same fashion until the seventh level. As the interaxial-distance reached its maximum, the zero-parallax distance was reduced until the final (tenth) level. In order to boost the number of depth cues in the scene, smaller copies of the focus object, in red, green and blue colors that were randomly assigned in equal likelihood, were scattered in the background. These copies were scaled slightly smaller, keeping the focus object as the center of attention.

3.2.3. Scene Complexity

We evaluated scene complexity in seven different levels, as follows. In the first level, the scene consisted of nothing but the focus object and the VE corridor. Then in the second level, 84 identical copies of the focus object, oscillating vertically in a sinusoidal pattern with a period of two seconds, were added along the left and right edges of the corridor. The third level

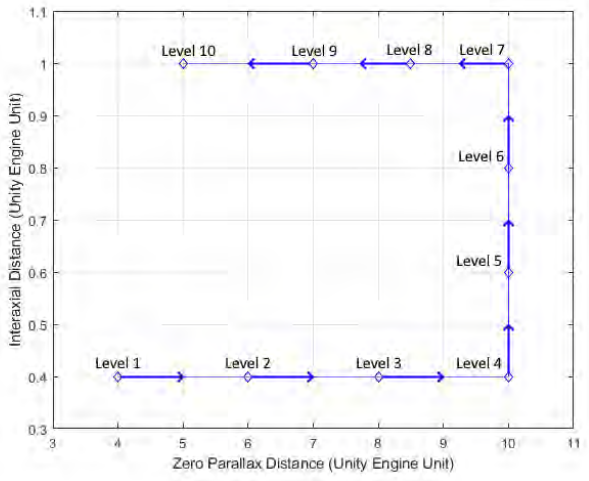

Figure 3: Directed chart showing the change of stereoscopic rendering parameters for each cue level.

Table 1: Table showing the parameter values (in Unity Engine units) used through the levels simulating stereoscopic rendering cues and the corresponding disparity values observed for the focus object (in number of pixels for frames rendered in a resolution of 1415 by 674 pixels). The separate row at the bottom gives the default values of the stereoscopic rendering parameters, which are used with the levels simulating the movement speed and scene complexity cues, and the corresponding disparity.

Cue Level	Interaxial Distance	Zero-Parallax Distance	Disparity
Level 1	0.400	4.0	175
Level 2	0.400	6.0	140
Level 3	0.400	8.0	106
Level 4	0.400	10.0	95
Level 5	0.600	10.0	137
Level 6	0.800	10.0	160
Level 7	1.000	10.0	213
Level 8	1.000	8.5	226
Level 9	1.000	7.0	253
Level 10	1.000	5.0	270
Default	0.022	10.0	105

further increased the number of objects by adding an additional 171 copies, forming three more lines along the corridor with increasing density towards the end. In the fourth level, these objects were randomly colored in red, green or blue, with equal likelihoods. The fifth level introduced particle emitters, which were attached to the objects added in the previous level and directed at the center and the camera. At this level, the emitters generated 20 particles per second matching the color of the source object. In the sixth level, the particles were given high dynamic range textures for intensified vividness and particle force fields were used to propel them directly at participants' center of view. Also, the emission rate was increased to 50 particles per second. Finally, the seventh level drastically increased the brightness of particles and boosted emission rate to 75 particles per second, resulting in particles occupying most of the field of view at severe discomfort.

In order to isolate the effects of varying complexity to the responses captured during the scene complexity trials, the other two scenes, simulating movement speed and stereoscopic rendering cues, were composed in minimal complexity. Likewise, we set the movement speed during the simulation of scene complexity and stereoscopic camera cues at the same minimum value (1.2 meters/sec) as the one in the first level of the movement speed scene. The supplementary video demonstrates a complete run of the three scenes comprising all simulated levels described above.

3.3. EEG Collection and Processing

To gather the EEG data, Emotiv Epoc+ [60], a saline-contact based headset, was used. The headset collects signals from 14 electrodes placed around the scalp according to the 10-20 standard. The data was recorded to the Emotiv Cloud service by a C# script using the Cortex API. The C# script was connected via TCP connection to the VR framework so that the markers could be added to EEG recordings to label the epochs. The connection also allowed to start recording from the framework, facilitating synchronization.

The three main kinds of information in EEG signals are spatial, temporal and spectral [61]. Spatial information corresponds to the location of the measured signals. The visual stimulus is first processed in the occipital lobe and then follows either a dorsal or ventral stream depending on its purpose [62]. Accordingly, among the fourteen available electrodes, we consider the data collected from the four electrodes closest to the occipital lobe, namely the O1 and O2 electrodes placed directly on the occipital lobe and the P7 and P8 electrodes placed on the parietal lobe.

A crucial step in an EEG feedback study is to determine the kind of effect that the brain activity to be explored has on the brain. A common practice is to make use of event-related potentials (ERPs), which are small, time-locked voltages that are generated by the brain in response to specific stimuli or events [63]. ERP can be reliably measured by averaging the responses recorded after a specific exposure repeated in a number of trials. However, oscillatory activities are not as easily detectable since they are associated with power changes in specific frequency bands, asynchronous and can be suppressed by noise. In this study, our aim is to explore the discomfort experienced in the VE that does not occur as a product of a particular momentary stimulus, but due to cumulative effects during exposure to varying stimuli. Therefore, here we adopt to evaluate the EEG data in terms of oscillatory activities as they are more apt for our purposes.

We used EEGLAB [64] for processing the EEG data. For the EEG recording of a single participant, three data files in EDF format, one recording for each session, were captured. Only 14 of the 39 channels stored in an EDF file actually carried data (electrical signals) from the scalp, and the others were concerned with contact quality, gyroscope measurements and markers. Hence, all channels except the ones carrying the data and the marker information were discarded. The corresponding marker values were imported to EEGLAB as events and the marker channel was then deleted as well, leaving only the 14 data channels.

Although Epoc+ provides notch filters at 50 and 60 Hz frequencies, we still encountered a heavy 50 Hz component during our inspection of the frequency domain response. Therefore, the time-series data was filtered using a 48 Hz low-pass filter and a higher order 1 Hz high-pass filter. Baseline removal was applied to the data, eliminating the mean of the entire recording and essentially making it a zero-mean signal.

Even though the filters eliminate part of the noise, some artifacts remain within the 1-48 Hz range. Most of these are the artifacts of eye movement, blink and miscellaneous muscle movements. Some of these artifacts can be removed using independent component analysis (ICA) [65, 66]. For this, the data was split into statistically independent components with ICA and the potential artifacts were eliminated automatically with ICLABEL [67], an independent component classifier trained with a dataset of expert labeled artifacts. Still, this process can not eliminate all remaining noise and artifacts since some components contain brain activity mixed with noise. After this step, the data was epoched accordingly (*i.e.*, separated into parts corresponding to the respective trials) and saved.

Spectral information is frequently used in brain-computer interface studies on oscillatory activities. For this, relative power changes in the selected frequency bands are considered. To extract the frequency information, first we compute the power spectral density (PSD) with Welch's method, giving the frequency-power information. To find the band power in a certain frequency band, PSD can be integrated across it. For our analysis, we used the relative powers of the bands θ = 4-8 Hz, α = 8-13 Hz, β = 13-25 Hz and γ = 25-45 Hz. The relative power is found as the percentage of the power from the selected band to the total power in the range of all considered bands. Then, to account for personal differences, the relative power captured during the baseline recording of the participant is subtracted to obtain *relative power change*.

We also make use of *signal magnitude area* (SMA) measure obtained from the processed EEG data as in [68]. While it is temporal in nature, SMA does not rely on synchronized markers as ERP. Hence, it bears potential to identify irregularities that may be missed by spectral analysis. SMA of each reading was acquired with the modified formula

$$SMA_{i-N/2} = \sum_{n=-N/2}^{N/2} |a_{i+n+1} - a_{i+n}| \quad (1)$$

which was used to create an SMA sequence from an EEG sample. This way of SMA calculation helps to emphasize inter-sample differences. Here, i denotes the SMA window position in the EEG reading and n denotes the index in the sample window. We used a window of $N = 256$ samples.

To detect spikes where EEG signal changed abruptly, a threshold was applied to the SMA output. The threshold was set to the mean and standard deviation of the SMA added together. When the SMA value exceeded this threshold for longer than 10 samples, it was counted as an *SMA event*. This process was repeated for the four electrodes (O1, O2, P7 and P8) under consideration. For data analysis, the difference between a participant's number of SMA events in a trial and number of SMA events in their baseline recording were used. A sample recording and its outputs for both SMA and thresholding are provided in Fig. 4.

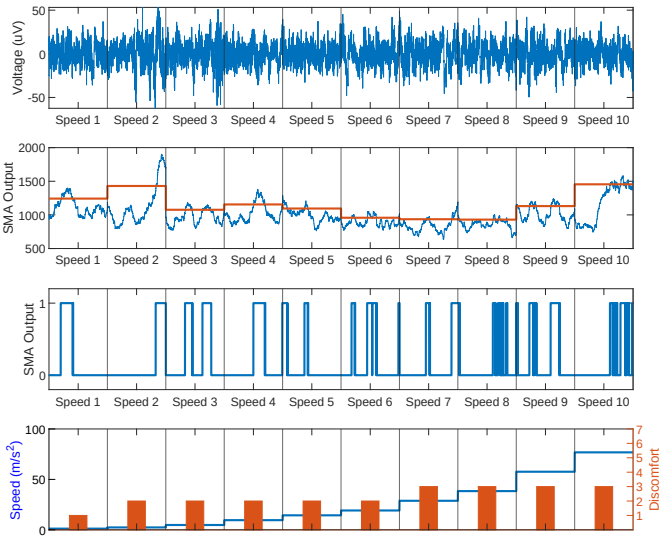

Figure 4: Plots showing both SMA and thresholding outputs for a sample EEG recording captured during the movement speed trials of a user in their second session. The change in the user's total SSQ score after the session was +41.14.

4. Results

The statistical analyses were conducted using JASP [69] to evaluate the relationship between stimulus factors, reported VR discomfort, and extracted EEG data based on the following hypotheses.

- The rise in persistent cybersickness increases with each session (H1)
- Immediate cybersickness reported during a session is linked to persistent cybersickness reported after that session (H2)
- Changes in the observed VR cues affect the level of immediate cybersickness (H3)
- Experience with VR, video gaming frequency and motion sickness susceptibility are predictive of the cybersickness felt (H4)
- Different cue types invoke cybersickness in different intensities (H5)
- EEG relative power changes are different for the cybersickness and non-cybersickness conditions. (H6)
- EEG relative power changes are linked to immediate cybersickness (H7)
- Different durations spent in the VE result in different EEG responses (relative power changes and SMA events) to cybersickness (H8)
- Different cues evoke different EEG responses (relative power changes and SMA events) to cybersickness (H9)

To evaluate the change in persistent cybersickness across the sessions, the differences between the consecutive SSQ responses were taken into account. As different participants were at different mental states at the beginning of the experiment, this approach aims to isolate the effect of the shown stimulus in the analysis. Once at the beginning of the experiment and once after each session, a participant reported a total of 4 SSQ responses. SSQ returns a total score (SSQ-T) in addition to three subscores corresponding to disorientation (SSQ-D), nausea (SSQ-N) and oculomotor discomfort (SSQ-O). The average changes in the SSQ scores after each session can be seen in Figure 5. A one way repeated measures analysis of variance (RMANOVA) applied to these changes rejected the null hypothesis for nausea, oculomotor and total scores as shown in Table 2. The averages show a definite increase for these three. However, it did not reject the null hypothesis for the changes in disorientation score (SSQ-D), indicating a linear behavior in increase, as Figure 5 illustrates.

In order to evaluate the effects of the simulated VR cues and personal factors (MSSQ percentile, level of VR experience and video gaming frequency) on immediate discomfort, we applied them into a linear regression model. For this, the movement speed and stereoscopic rendering parameters were entered as given in Sections 3.2.1 and 3.2.2, respectively, while scene complexity was entered by the corresponding level number ranging from 1 to 7. The data was separated by sessions to account for the time spent in VR. The adjusted R^2 metric of re-

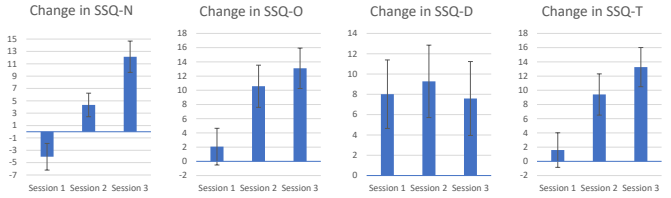

Figure 5: Changes in the SSQ scores following each session. The error bars represent ± 1 standard error.

Table 2: Average changes in SSQ scores per session and corresponding RMANOVA test results.

	Session 1	Session 2	Session 3	Significance
Nausea Difference	-4.04 ± 12.40	4.43 ± 10.95	12.14 ± 14.56	$F_{2,64}$ = 12.558, **p < 0.001**
Oculomotor Difference	2.06 ± 14.83	10.56 ± 17.04	13.09 ± 16.33	$F_{2,64}$ = 4.283, **p = 0.018**
Disorientation Difference	8.01 ± 19.38	9.28 ± 20.49	7.59 ± 20.90	$F_{2,64}$ = 0.053, p = 0.949
SSQ-Total Difference	1.59 ± 13.99	9.40 ± 16.67	13.26 ± 15.84	$F_{2,64}$ = 4.728, **p = 0.012**

gression models and individual values (β and p) are provided in Table 3. Adjusted R^2 metric increases over successive sessions, indicating the regression model gets better at expressing the relationship between the IDS and personal/controlled factors with more time spent in VR. All three VR cues are indicated to be significant predictors across all sessions. Similarly, MSSQ percentile is also significant across all sessions. While level of VR experience is a significant predictor in sessions 1 and 3, video gaming habits are identified significant in sessions 1 and 2.

Correlations between per-session averages of IDS and changes in SSQ scores were investigated to explore the relationship between immediate and persistent cybersickness. Weak yet significant correlations were found between the IDS averages of the speed trials and changes in SSQ-N (r = 0.210, p = 0.037), SSQ-O (r = 0.223, p = 0.027) and SSQ-T (r = 0.230, p = 0.022). A similar link between SSQ-N changes and the average IDSs of the stereoscopic cue levels was also observed (r = 0.273, p = 0.027).

Table 3: Statistics of the linear regression models that take controlled and personal factors as input and attempt to predict IDS separated by session. Adjusted R^2 metric, ranging from 0 to 1, describes how well the model predicts the output. β is the standardized coefficient for the corresponding input. Inputs with p values less than 0.05 were considered statistically significant predictors for the immediate discomfort and shown in bold.

	Session 1	Session 2	Session 3
Adjusted R^2	R^2 = 0.238	R^2 = 0.244	R^2 = 0.309
MSSQ Percentile	**β = 0.192 p < 0.001**	**β = 0.136 p < 0.001**	**β = 0.145 p < 0.001**
VR Experience	**β = 0.184 p < 0.001**	β = 0.019 p = 0.517	**β = -0.105 p < 0.001**
Video Gaming Frequency	**β = -0.106 p = 0.001**	**β = -0.150 p < 0.001**	β = -0.035 p = 0.264
Scene Complexity	**β = 0.314 p < 0.001**	**β = 0.396 p < 0.001**	**β = 0.320 p < 0.001**
Movement Speed	**β = 0.257 p < 0.001**	**β = 0.289 p < 0.001**	**β = 0.273 p < 0.001**
Camera Interaxial-Distance	**β = 0.372 p < 0.001**	**β = 0.355 p < 0.001**	**β = 0.514 p < 0.001**
Camera Zero-Parallax Distance	**β = 0.075 p = 0.028**	**β = 0.089 p = 0.009**	**β = 0.076 p = 0.019**

To evaluate whether different VR cues lead to different IDSs, a two-way RMANOVA with Greenhouse-Geisser correction was applied to participants' average IDSs, separated by both cue type and session. The RMANOVA test rejected the null hypothesis for both cue type ($F_{1.27,40.68}$ = 8.87, p < 0.01), and session ($F_{1.52,48.08}$ = 5.80, p = 0.01), as well as their interaction effects ($F_{3.20,102.48}$ = 6.07, p < 0.001). Main effect analysis was performed for both cue type and session difference. All sessions showed significant differences for cue types (for session 1: F_2 = 3.72, p < 0.05; for session 2: F_2 = 4.35, p < 0.05; and for session 3: F_2 = 16.83, p < 0.001). However, for the session main effect, only the IDS responses to the stereoscopic rendering cues indicated a significant change (F_2 = 13.07, p < 0.001) while the scores associated with scene complexity (F_2 = 1.21, p = 0.305) and speed (F_2 = 1.11, p = 0.335) cues did not change significantly. The averages of the reported IDSs as separated by cues and sessions are given in Figure 6.

We evaluated the relative power changes in the frequency bands of the O1, O2, P7 and P8 electrodes, returning sixteen spectral measures per stimulus level experienced by each participant. First, the changes in these frequency bands were inspected to assess the relationships between different levels of cue types and the acquired EEG data. The standardized average of the relative power changes in the four frequency bands of the specified electrodes against the cue types and levels are shown in the top three rows of Figure 7. For each frequency band, the standardized relative power changes from the four electrodes are averaged and shown in the bottom three rows of Figure 7. The relative power changes in the theta frequency band exhibit an upwards trend as the stimulus levels progress, especially for the movement speed and stereoscopic rendering cues. The relative power changes in the alpha and beta frequency bands do not present a set trend but strong variations are seen in the alpha band across certain levels that can indicate a sudden change of discomfort between those levels. It is also seen that standardized relative power change in the gamma band exhibits a downwards trend as the stereoscopic rendering levels progress.

Correlations between IDS and EEG features are given in Table 4. Analysis reveals that the stereoscopic cues from session 3 bear low correlation despite seeing a high amount of discomfort. Further evaluation shows that the ratio of levels with reported discomfort is relatively high for the stereoscopic cues at session 3 (54% of 330 levels recorded from all participants). The data was also evaluated with Welch's t-test, revealing multiple significant differences between the discomfort and non-discomfort conditions with no apparent significant correlations. Relative power changes for O1 theta band (t = -2.704, p

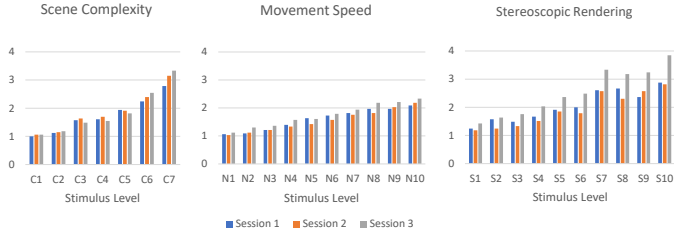

Figure 6: Average IDS per session, separated by cue type.

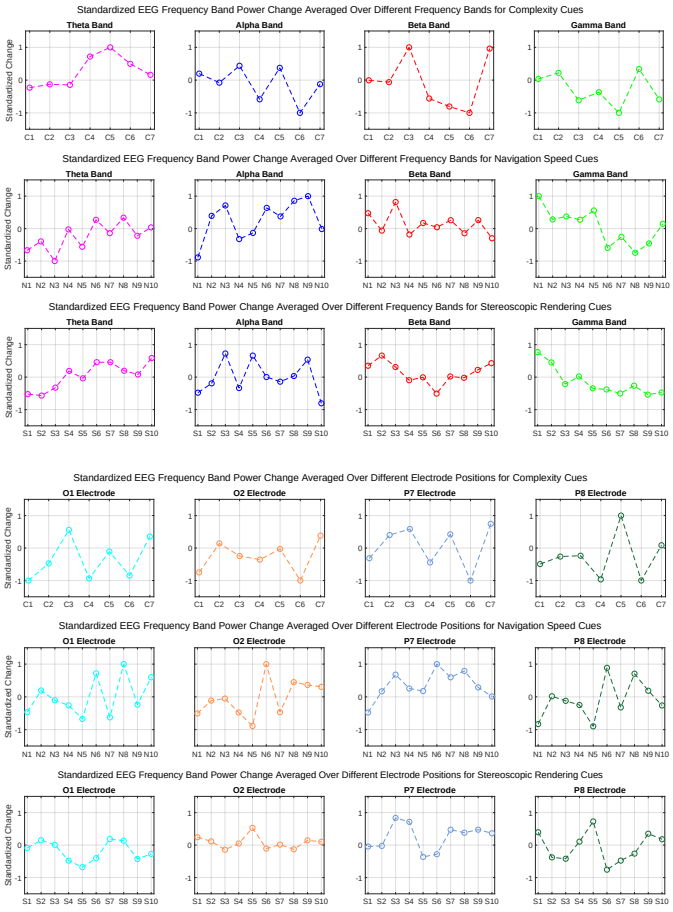

Figure 7: Standardized EEG relative power changes averaged over different frequency bands separated by cue type across all sessions (top half) and over different electrode positions separated by cue type across all sessions (bottom half).

= 0.008), O2 theta band (t = -3.301, p < 0.001), P7 theta band (t = -2.754, p = 0.007), P7 alpha band (t = -2.047, p = 0.043) and P8 theta band (t = -2.516, p = 0.013) show significantly higher values for the discomfort condition. Relative power changes for O1 beta band (t = 3.280, p < 0.001), O1 gamma band (t = 1.989, p = 0.049), O2 beta band (t = 3.949, p < 0.001), O2 gamma band (t = 2.635, p = 0.009), P7 beta band (t = 4.035, p < 0.001), P7 gamma band (t = 2.813, p = 0.006), P8 gamma band (t = 2.012, p = 0.046) show significantly lower values for the discomfort condition.

Mean EEG relative power changes per session were compared to the SSQ changes of the corresponding sessions by Pearson's correlation analysis. Within the correlations of 16 x 4 variables, the Pearson's analysis revealed 17 significant correlations. The whole set of correlation results are given in Table 5.

We also investigated the use of IDS as a binary measure indicating cybersickness and non-cybersickness conditions. For this purpose, the trials were split across different cues. After this, Welch's t-test was applied between trials with discomfort and no discomfort. The test shows multiple significant results, most notably for the movement speed cues. Results are given in Table 6.

In order to check whether discomfort from different cues evoke different responses in EEG that can be detected from the relative power change, two-way multivariate ANOVA (MANOVA) was applied to the stimulus levels where discomfort is present, testing for evident differences in EEG relative power changes for different cues and sessions. The MANOVA analysis did not reject the null hypothesis for different cues ($F_{2,1284}$) = 1.239, p = 0.168); but revealed that the EEG relative power change from baseline shows a significant difference for different sessions ($F_{2,1284}$ = 7.778, p < 0.001) and a significant interaction effect ($F_{4,1284}$ = 1.705, p < 0.001). Cue effect on the EEG relative power changes was further investigated with individual ANOVA tests which exhibited that the relative power changes of several electrode-frequency band pairs show significant differences across different cue conditions. The results are provided in Table 7.

Similarly, we explored the effects of different cues and time spent in VR on the EEG response to cybersickness in the form of SMA events. Again, only the trials reporting cybersickness were included in the analysis. Two separate two-way MANOVA tests were employed, one investigating specific elec-

Table 4: Pearson's correlation analysis results between participants' IDS and the EEG relative power changes divided by sessions and cue type.

	Session 1			Session 2			Session 3		
EEG Relative Power Change (%)	Complexity	Speed	Stereoscopic	Complexity	Speed	Stereoscopic	Complexity	Speed	Stereoscopic
O1 theta	**0.163***	**0.160****	0.068	**0.177****	**0.150****	**−0.124***	0.021	0.012	0.040
O1 alpha	0.045	**0.297*****	−0.061	−0.022	**0.126***	0.025	**−0.152***	**−0.165****	−0.051
O1 beta	−0.115	−0.097	−0.047	**−0.133***	**−0.113***	**0.160****	0.057	**0.145****	−0.045
O1 gamma	**−0.174****	**−0.294*****	−0.022	**−0.162***	**−0.246*****	0.038	0.015	0.006	0.005
O2 theta	0.122	**0.111***	0.026	**0.168***	**0.155****	**−0.117***	0.028	0.054	0.079
O2 alpha	0.014	**0.197*****	0.000	−0.126	0.007	−0.051	**−0.149***	**−0.177****	−0.035
O2 beta	−0.010	**−0.135***	0.028	−0.071	−0.049	0.092	0.059	0.091	−0.075
O2 gamma	**−0.136***	**−0.162****	−0.066	−0.088	**−0.194*****	**0.135***	0.022	−0.006	−0.058
P7 theta	**0.150***	**0.291*****	0.057	**0.162***	**0.159****	**−0.171****	−0.005	0.003	0.041
P7 alpha	**0.131***	**0.295*****	−0.042	−0.005	0.086	−0.029	−0.088	−0.024	0.099
P7 beta	−0.110	**−0.179****	−0.024	−0.045	−0.085	**0.197*****	0.015	0.030	−0.087
P7 gamma	**−0.184****	**−0.368*****	−0.048	**−0.206****	**−0.224*****	**0.111***	0.041	−0.009	−0.050
P8 theta	**0.171****	**0.223*****	**0.108***	**0.146***	**0.177****	**−0.121***	0.017	0.046	0.044
P8 alpha	−0.001	**0.133***	−0.019	−0.066	0.053	**−0.136***	**−0.228*****	**−0.242*****	**−0.113***
P8 beta	−0.075	**−0.119***	**−0.114***	−0.045	−0.103	**0.138***	0.083	**0.147****	0.022
P8 gamma	**−0.151***	**−0.274*****	−0.064	−0.120	**−0.207*****	**0.161****	0.071	0.022	−0.013

* p < 0.05, ** p < 0.01, *** p < 0.001

Table 5: Correlation analysis results between SSQ scores and EEG relative power changes.

	Changes in Simulator Sickness Questionnaire Scores			
EEG Relative Power Change (%)	Nausea	Oculomotor	Disorientation	Total
O1 theta	0.062	**0.257***	0.167	**0.208***
O1 alpha	0.103	0.047	0.130	0.103
O1 beta	−0.085	−0.190	−0.158	−0.179
O1 gamma	−0.161	**−0.289****	**−0.262****	**−0.279****
O2 theta	0.045	**0.260****	0.194	**0.212***
O2 alpha	0.114	0.016	0.045	0.063
O2 beta	−0.117	−0.197	−0.116	−0.179
O2 gamma	−0.098	**−0.263****	**−0.247***	**−0.250***
P7 theta	0.031	**0.226***	0.116	0.164
P7 alpha	0.123	0.049	0.115	0.106
P7 beta	−0.035	**−0.200***	−0.138	−0.160
P7 gamma	−0.092	**−0.212***	−0.154	−0.191
P8 theta	0.056	**0.225***	0.137	0.180
P8 alpha	0.165	0.015	0.146	0.113
P8 beta	−0.094	−0.178	−0.154	−0.174
P8 gamma	−0.126	**−0.218***	**−0.207***	**−0.223***

* p < 0.05, ** p < 0.01, *** p < 0.001

Table 6: T-test results (t values) for EEG relative power changes between the trials that reported discomfort and the trials that reported no discomfort. The results are split across different cues. Significant results are indicated with asterisks. Positive t values indicate that trials where discomfort was reported return lower relative power changes than trials without discomfort, while negative t values indicate the opposite.

EEG Relative Power Change (%)	Complexity	Speed	Stereoscopic
O1 theta	**−3.029****	**−2.854****	−1.869
O1 alpha	1.655	−1.865	**2.116***
O1 beta	1.203	0.775	1.393
O1 gamma	**2.651****	**4.985*****	0.395
O2 theta	**−2.853****	**−3.011****	−1.841
O2 alpha	**2.447***	−1.206	**2.138***
O2 beta	1.236	1.018	**2.186***
O2 gamma	1.314	**4.192*****	−0.065
P7 theta	**−2.297***	**−3.759*****	−0.341
P7 alpha	0.206	**−3.553*****	−0.140
P7 beta	**2.284***	**2.364***	0.875
P7 gamma	**1.988***	**5.427*****	0.307
P8 theta	**−2.337***	**−3.747*****	−1.901
P8 alpha	**2.013***	−0.520	**3.413*****
P8 beta	1.032	0.761	0.663
P8 gamma	1.081	**4.557*****	0.123

* p < 0.05, ** p < 0.01, *** p < 0.001

Table 7: Average relative power changes for discomfort condition separated by different cues and their corresponding ANOVA results. The table includes only the electrode-frequency band pairs that returned a significant p-value less than 0.05 in the ANOVA test.

	Complexity M ± SD	Speed M ± SD	Stereoscopic M ± SD	Significance
Alpha Relative Power Change of Electrode O1	-3.21 ± 8.86	-1.61 ± 9.36	-2.94 ± 9.53	$F_{2,1284} = 3.264$ **p = 0.039**
Gamma Relative Power Change of Electrode O1	3.20 ± 11.99	3.11 ± 11.05	4.78 ± 11.20	$F_{2,1284} = 3.184$ **p = 0.042**
Alpha Relative Power Change of Electrode O2	-5.13 ± 9.85	-2.95 ± 9.43	-4.49 ± 10.23	$F_{2,1284} = 4.772$ **p = 0.009**
Gamma Relative Power Change of Electrode O2	4.19 ± 12.16	3.26 ± 10.69	5.38 ± 11.40	$F_{2,1284} = 4.129$ **p = 0.016**
Alpha Relative Power Change of Electrode P7	-1.24 ± 6.74	-0.13 ± 6.94	-1.23 ± 6.73	$F_{2,1284} = 3.577$ **p = 0.028**
Alpha Relative Power Change of Electrode P8	-2.06 ± 7.77	-0.74 ± 8.20	-1.87 ± 7.69	$F_{2,1284} = 3.210$ **p = 0.041**

trodes (O1, O2, P7 and P8) and another investigating the regions (occipital and parietal) encompassing these electrodes. The test investigating the electrodes returned a significant effect of time spent in VR ($F_{2,1284} = 9.314$, $p < 0.001$), however did not reject the null hypothesis for different cues ($F_{2,1284} = 1.333$, $p = 0.222$) nor the interaction effect ($F_{4,1284} = 1.492$ and $p = 0.093$). Similarly, the test regarding the different regions returned significant results for session effect ($F_{2,1284} = 8.536$, $p < 0.001$), but did not for different cues ($F_{2,1284} = 2.148$, $p = 0.072$) or the interaction effect ($F_{4,1284} = 1.314$ and $p = 0.232$). Individual ANOVA testing for sessions, given in Table 8, reported significant results for all electrodes and regions except the P7 electrode, while the ANOVA for different cues did not return significant results.

Table 8: Main statistics of the detected SMA events per-session in trials with discomfort condition and the corresponding ANOVA results (rightmost column).

	Session 1 M ± SD	Session 2 M ± SD	Session 3 M ± SD	Significance
O1 Electrode	0.64 ± 2.6	0.22 ± 2.55	0.12 ± 3.23	$F_{2,1284} = 4.037$ **p = 0.018**
O2 Electrode	0.64 ± 2.49	-0.09 ± 2.75	0.26 ± 2.90	$F_{2,1284} = 7.324$ **p < 0.001**
P7 Electrode	0.58 ± 2.57	0.73 ± 2.26	0.80 ± 2.34	$F_{2,1284} = 0.954$ p = 0.386
P8 Electrode	0.88 ± 2.63	-0.18 ± 2.87	0.91 ± 2.43	$F_{2,1284} = 23.265$ **p < 0.001**
Occipital Region	1.28 ± 4.28	0.125 ± 4.25	0.38 ± 4.69	$F_{2,1284} = 7.699$ **p < 0.001**
Parietal Region	1.46 ± 4.35	0.55 ± 4.17	1.72 ± 3.77	$F_{2,1284} = 9.629$ **p < 0.001**

Additionally, curves of the averages for the number of SMA events and IDS through the levels are provided in Figure 8. The number of events in the occipital region is seen to decrease after the first session, especially for the complexity and stereoscopic rendering cues. On the other hand, the number of events in the parietal region exhibits a similar pattern after the first session, but then rises in the third session for all cues, a trend that can also be seen in Table 8. Nevertheless, as seen in Figure 8, the averages for the number of SMA events do not illustrate clear trends with respect to the changes in simulated cue levels.

5. Discussion

Investigating the first hypothesis (H1:"The rise in persistent cybersickness increases with each session"), a growing per-session increase in cybersickness measured by SSQ scores was observed through the experiment except the disorientation subscore, which had a reduced rise in the last session. Hence, the hypothesis is confirmed for total sickness and SSQ subscores related to nausea and oculomotor strain but not for disorientation. This finding is in line with multiple previous studies [45, 70, 41] that identified time spent immersed in VR as an important factor in cybersickness, reporting increased discomfort with prolonged use. As disorientation subscore measures the severity of symptoms such as dizziness and vertigo, one reason behind its trend can be that the participants might have felt these symptoms much earlier than the symptoms associated with nausea or oculomotor subscores.

The analysis exploring the link between immediate cybersickness reported in-VR and persistent cybersickness reported post-VR (H2) revealed significant correlations between the

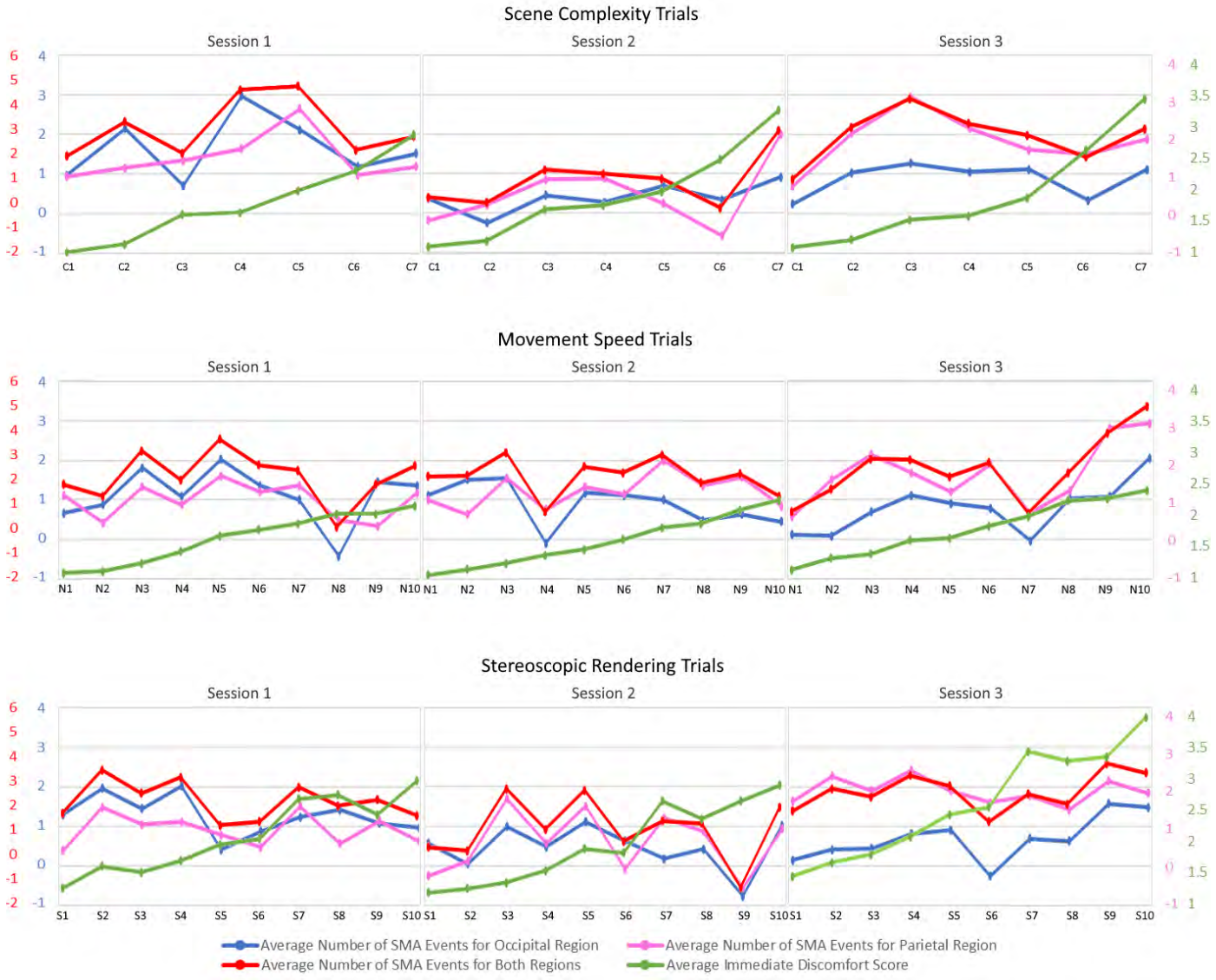

Figure 8: Curves representing average number of SMA events and IDS, separated by cue type and session. To ease examination, all graphs use the same vertical scale.

immediate discomfort experienced with the speed cues and changes in total SSQ scores. Therefore, the results confirm H2 for the cybersickness invoked by the speed cues but not for the other two.

For all three sessions, scene parameters were found as significant predictors for immediate cybersickness. Similarly, MSSQ percentile turned out to be a significant predictor across all sessions with a positive coefficient, affirming the assumption that people who are more susceptible to motion sickness would be more susceptible to cybersickness as well. Video gaming frequency was identified as a significant predictor for the first two sessions with a negative coefficient, suggesting gamers could be less prone to feeling discomfort with VR-HMDs for a certain duration, however this tolerance seems to wear off with prolonged uses as seen in session 3 with video gaming frequency showing no significant effect. VR experience level of the participant shows a mixed effect by emerging as a significant predictor for sessions 1 and 3 with opposing coefficients (negative on session 1 and positive on session 3). This may indicate that the participants with more VR experience could be better at accommodating to cybersickness and feel less discomfort in longer sessions. Another noteworthy point is that interaxial-distance, a key stereoscopic rendering parameter, seems to have contributed more to discomfort in session 3 than session 1. This is in line with the findings of Wang et al. [71] that the ability of accommodation decreased with repeated exposure to VAC-inducing content. This probably causes the same stimulus to be more taxing for the human visual system, generating greater discomfort and further visual fatigue. All in all, while hypothesis H3 (“Changes in the observed VR cues affect the level of immediate cybersickness.”) is fully confirmed, H4 (“Experience with VR, video gaming frequency and motion sickness susceptibility are predictive of the cybersickness felt.”) is partially confirmed due to VR experience and video gaming fre-

quency not being significant predictors for all sessions.

Immediate discomfort was found to have changed significantly for both different sessions and different cues. Main effect analysis showed that different cues led to different grades of immediate discomfort in all sessions, however only the immediate discomfort in response to the stereoscopic rendering cue levels showed a significant change across different sessions. Again, this is in line with Wang et al.'s findings [71]. As different cues consistently resulted in different immediate discomfort, hypothesis H5 ("Different cue types invoke cybersickness in different intensities.") is confirmed.

EEG feedback revealed weak but significant correlations between relative power changes, primarily in the theta and gamma frequency bands, and persistent cybersickness scores. Theta and gamma frequency relative power changes from all four electrodes showed significant correlations with the oculomotor subscores. In addition, gamma band relative power changes for O1, O2 and P8 electrodes correlated significantly with the total SSQ scores as well as the disorientation subscores. The nausea subscore was not found to correlate significantly with any electrode-frequency band pairs. These results show gamma frequency relative power change to be an especially valuable metric when it comes to long term effects of cybersickness. This complies with Jang et al.'s [44] results, which showed lower beta and gamma absolute bandpowers for the user group with higher SSQ scores.

Evaluation of the t-test results for relative power changes allowed us to examine the IDS as a binary measure. The tests revealed increased theta relative power change for both complexity and speed cues for the discomfort condition. Alpha frequency relative power change was found to be increasing for speed cues, however showed a decrease for stereoscopic and complexity cues for trials with discomfort. Beta relative power change was found to be decreasing for all cues. However, the t-test yielded significant results only for the O2 electrode for stereoscopic cues and the P7 electrode for the speed and complexity cues. Gamma relative power change showed a significant decrease for complexity and speed trials with discomfort as well. The effect seen on the theta and alpha frequency bands in speed cues are also reported by Nurnberger et al. [45]. Similarly, the effect on the beta and gamma frequency bands is in line with multiple works [34, 44]. These results partially confirm hypothesis H6 ("EEG relative power changes are different for the cybersickness and non-cybersickness conditions.") as significant differences are observed between certain EEG relative power changes for trials with and without reports of discomfort.

Regarding the correlation between immediate discomfort and EEG data, the results associated with the complexity and speed cues were found to be consistent with the SSQ correlations. The significant correlations are mainly seen on the theta and gamma frequency bands. Relative power changes in the alpha and beta frequency bands are also seen to be correlated with certain electrode positions. However, discomfort due to stereoscopic rendering cues led to varying responses across the three sessions. The first session results show little relationship between EEG relative power changes and IDSs. While the second session results revealed more significant correlations, these were not in line with the corresponding SSQ correlations. The third session revealed a low amount of significant correlations, similar to the first session; yet, the t-tests revealed multiple electrode-frequency band pairs that showed significantly different relative power changes between the discomfort and non-discomfort conditions. The t-test results were also consistent with the correlations observed between SSQ and relative power changes. The significant differences demonstrated by the t-tests, despite the lack of correlations, may indicate that it is possible to observe the presence of discomfort in the EEG response interpreted with the relative power change measure, but not the intensity of it. Altogether, these findings confirm hypothesis H7 ("EEG relative power changes are linked to immediate cybersickness.") only partially.

The effects of different cues and sessions on EEG relative power changes from the levels where discomfort is present was tested. While the MANOVA test did not return a significant effect for the cue type, individual ANOVA tests showed that alpha and gamma relative power changes of certain electrodes exhibited different responses for different cues across all sessions. These features are specifically important to identify the source of cybersickness experienced by the user. Similarly, Lin et al. showed alpha and gamma bands of the EEG power spectrum as valid indicators of motion sickness [72]. While the number of SMA events returned similar results, there was no indication of a cue dependent response with this metric. The hypothesis H8 ("Different durations spent in the VE result in different EEG responses to cybersickness.") is fully confirmed as the MANOVA tests regarding both the relative power changes and the number of SMA events rejected the null hypothesis for different sessions. However, the hypothesis H9 ("Different cues evoke different EEG responses to cybersickness.") is confirmed partially for relative power changes as the MANOVA results for relative power changes rejected the null hypothesis for different cues, but individual ANOVA testing returned some significant results. The hypothesis H9 is rejected outright for SMA events due to the absence of supporting MANOVA and individual ANOVA results.

6. Limitations

Although analysing the brain feedback in terms of oscillatory activities provided us with rich data of the vision-related accumulated brain response to the simulated VR stimuli, oscillatory activities are seriously challenged by noise and other artifacts which do not pose such problems in ERP analysis by means of precisely-timed measurements and averaging after many repeated trials of the exact same stimuli. Further, the EEG data captured during our study inevitably incorporated noise and other artifacts in addition to the actual response, mainly due to the fact that the participants were given the liberty to look around in accordance with the free-viewing paradigm as they were asked to follow the focus object during the trials. Their head and eye movements that occurred while looking around introduced unwanted artifacts in the received EEG signals. Although the application of the widely-used mitigation measures

of EEG preprocessing filtered out most of these, it is not possible to remove all completely and the remaining artifacts eventually may have had some effect on the evaluation.

The user study design was subject to limitations, as well. Some of these limitations are due to the VE design decisions with the intent of minimizing other EEG artifacts. For instance, the VE was kept as simple as possible in order to prevent possible emotional response, among others. Nonetheless, the simple hall environment and the movement down this straight hall might have had a limiting impact on the VE's ability to elicit vection. On the other hand, while more twists and turns in the movement path, as done with roller-coasters in some of the previous cybersickness studies [23, 32], would likely cause more discomfort, they would also cause more head movements, which introduce EEG artifacts, and would not be suitable for our study where we aim to investigate the effects of separate VR cues in isolation from other factors. Another limitation is that our user study design lacks a designated control condition. However, we use the EEG recordings captured during the baseline scene as reference. Furthermore, while having back-to-back sessions with three-minute breaks in-between was a deliberate experimental design choice to enable the investigation of time-related accumulation effects on cybersickness, the durations of the break periods between consecutive levels and scenes can be regarded as limiting to a certain extent. To avoid contamination effects, before starting a new scene, participants were asked if they were comfortable continuing the experiment at the end of the designated amount of time. Also, they were instructed that they should resume the experiment by clicking the designated hand controller button if and only if they felt ready after any break following a level or a scene. While such precautions have been utilized in previous cybersickness studies using multiple short-term stimuli in a row [37, 73, 74], as in our study, we should note that these measures may not have been fully sufficient to completely eliminate intra-stimulus contamination.

7. Conclusion

In this study, we have presented a broad evaluation of the effects of the movement speed, scene complexity and stereoscopic rendering cues on cybersickness experienced with VR-HMDs through a user study where we collected EEG feedback from 33 participants with corresponding self-reported discomfort measures. The supplementary video illustrates the scenes along with the standardized EEG relative power changes for the corresponding stimulus levels.

Analysis of EEG features and self-reports of discomfort revealed connections that indicate a relationship between EEG data and the presence of cybersickness for all three cue types. Persistent cybersickness was found to be connected to immediate cybersickness invoked by the speed cues. Similarly, immediate cybersickness was shown to be affected by the changes in VR cues. EEG relative power changes were also found to be linked to both immediate and persistent cybersickness, especially in the theta and gamma frequency bands. We also observed significantly different EEG relative power changes between when participants reported and did not report cybersickness. Further, these significant differences were present in the lack of correlations, hinting that EEG relative power changes can reveal the presence of cybersickness but not the intensity.

The amount of increase in total persistent cybersickness, as well as the amount of increase in persistent nausea and oculomotor discomfort, grew with each session spent immersed in VR. Also, immediate discomfort for stereoscopic rendering cues and the observed EEG markers (relative power changes and number of SMA events) showed a definite change with further sessions. The increase in immediate cybersickness in response to the stereoscopic rendering cues over successive sessions suggests that the tolerance to these effects may be decrease over time. Additionally, immediate cybersickness and the EEG relative power changes in certain electrode-frequency band pairs, especially the ones associated with the alpha band, were significantly different for different VR cues.

EEG data has been shown to be beneficial for cybersickness analysis via neural networks [75, 76, 77] as they can infer relationships between signals from different electrodes and evaluate the spatial response along with other features that can be extracted from the time series data. The data acquired with the study show the presence of cybersickness and that the causing stimuli can have significantly distinct EEG responses, hypothetically allowing for advancing the future work in terms of both detecting cybersickness and classifying the cause of it for proper mitigation. Further, findings of this study can act as guidelines for future work on cybersickness research with EEG feedback.

Declarations

Data Availability. The data collected and analysed for this work is available at the paper website.

Code availability. The code used to process the data is available at the paper website.

Funding. This work was supported by the Scientific and Technical Research Council of Turkey (TUBITAK, project grant number 116E280).

Conflicts of interest/Competing interests. The authors declare that they have no known competing financial interests or personal relationships that could have appeared to influence the work reported in this paper.

Ethics approval. This study has been approved by Hacettepe University Ethics Board.

Consent to participate. Written informed consent was obtained from all individuals participated in this study.

Consent for publication. The participants consented to the publication of their collected data without identifying information.

References

[1] J.J. LaViola Jr, A discussion of cybersickness in virtual environments, ACM SIGCHI Bulletin 32 (2000) 47–56.

[2] S. Martirosov, M. Bures, T. Zitka, Cyber sickness in low-immersive, semi-immersive, and fully immersive virtual reality, Virtual Reality 26 (2022) 15–32.

[3] L. Rebenitsch, C. Owen, Estimating cybersickness from virtual reality applications, Virtual Reality 25 (2021) 165–174.
[4] L. Rebenitsch, C. Owen, Review on cybersickness in applications and visual displays, Virtual Reality 20 (2016) 101–125.
[5] C.L. Liu, S.T. Uang, Effects of presence on causing cybersickness in the elderly within a 3d virtual store, in: International Conference on Human-Computer Interaction, Springer, 2011, pp. 490–499.
[6] U. Celikcan, Applications of virtual reality in education and medicine: A review of the past, present, and future outlook, Dicle Üniversitesi Mühendislik Fakültesi Mühendislik Dergisi 13 (2022) 235 – 251.
[7] A.S. Fernandes, S.K. Feiner, Combating vr sickness through subtle dynamic field-of-view modification, in: 2016 IEEE symposium on 3D user interfaces (3DUI), IEEE, 2016, pp. 201–210.
[8] E. Chang, I. Hwang, H. Jeon, Y. Chun, H.T. Kim, C. Park, Effects of rest frames on cybersickness and oscillatory brain activity, in: 2013 International Winter Workshop on Brain-Computer Interface (BCI), IEEE, 2013, pp. 62–64.
[9] D.M. Hoffman, A.R. Girshick, K. Akeley, M.S. Banks, Vergence–accommodation conflicts hinder visual performance and cause visual fatigue, Journal of vision 8 (2008) 33–33.
[10] A. Szpak, S.C. Michalski, D. Saredakis, C.S. Chen, T. Loetscher, Beyond feeling sick: The visual and cognitive aftereffects of virtual reality, IEEE Access 7 (2019) 130883–130892.
[11] P. Caserman, A. Garcia-Agundez, A. Gámez Zerban, S. Göbel, Cybersickness in current-generation virtual reality head-mounted displays: systematic review and outlook, Virtual Reality 25 (2021) 1153–1170.
[12] U. Celikcan, G. Cimen, E.B. Kevinc, T. Capin, Attention-aware disparity control in interactive environments, The Visual Computer 29 (2013) 685–694.
[13] R.S. Kennedy, N.E. Lane, K.S. Berbaum, M.G. Lilienthal, Simulator sickness questionnaire: An enhanced method for quantifying simulator sickness, The international journal of aviation psychology 3 (1993) 203–220.
[14] S.L. Ames, J.S. Wolffsohn, N.A. Mcbrien, The development of a symptom questionnaire for assessing virtual reality viewing using a head-mounted display, Optometry and Vision Science 82 (2005) 168–176.
[15] M.L. van Emmerik, S.C. de Vries, J.E. Bos, Internal and external fields of view affect cybersickness, Displays 32 (2011) 169–174.
[16] M. Pouke, A. Tiiro, S.M. LaValle, T. Ojala, Effects of visual realism and moving detail on cybersickness, in: 2018 IEEE Conference on Virtual Reality and 3D User Interfaces (VR), IEEE, 2018, pp. 665–666.
[17] U. Celikcan, Detection and mitigation of cybersickness via eeg-based visual comfort improvement, in: 2019 3rd International Symposium on Multidisciplinary Studies and Innovative Technologies (ISMSIT), IEEE, 2019, pp. 1–4.
[18] M. Zhou, C. Tian, R. Cao, B. Wang, Y. Niu, T. Hu, H. Guo, J. Xiang, Epileptic seizure detection based on eeg signals and cnn, Frontiers in neuroinformatics 12 (2018) 95.
[19] V.J. Lawhern, A.J. Solon, N.R. Waytowich, S.M. Gordon, C.P. Hung, B.J. Lance, Eegnet: a compact convolutional neural network for eeg-based brain–computer interfaces, Journal of neural engineering 15 (2018) 056013.
[20] E.M. Kolasinski, Simulator Sickness in Virtual Environments., Technical Report, Army research Inst for the behavioral and social sciences Alexandria VA, 1995.
[21] N. Tian, P. Lopes, R. Boulic, A review of cybersickness in head-mounted displays: raising attention to individual susceptibility, Virtual Reality (2022) 1–33.
[22] T. Porcino, D. Trevisan, E. Clua, A cybersickness review: causes, strategies, and classification methods, Journal on Interactive Systems 12 (2021) 269–282.
[23] S. Wibirama, H.A. Nugroho, K. Hamamoto, Depth gaze and ecg based frequency dynamics during motion sickness in stereoscopic 3d movie, Entertainment computing 26 (2018) 117–127.
[24] B. Keshavarz, A.E. Philipp-Muller, W. Hemmerich, B.E. Riecke, J.L. Campos, The effect of visual motion stimulus characteristics on vection and visually induced motion sickness, Displays 58 (2019) 71–81.
[25] K.K. Kwok, A.K. Ng, H.Y. Lau, Effect of navigation speed and vr devices on cybersickness, in: 2018 IEEE International Symposium on Mixed and Augmented Reality Adjunct (ISMAR-Adjunct), IEEE, 2018, pp. 91–92.
[26] R.H. So, W. Lo, A.T. Ho, Effects of navigation speed on motion sickness caused by an immersive virtual environment, Human factors 43 (2001) 452–461.
[27] R.H. So, A. Ho, W. Lo, A metric to quantify virtual scene movement for the study of cybersickness: Definition, implementation, and verification, Presence 10 (2001) 193–215.
[28] S. Palmisano, R. Mursic, J. Kim, Vection and cybersickness generated by head-and-display motion in the oculus rift, Displays 46 (2017) 1–8.
[29] J. Kim, W. Luu, S. Palmisano, Multisensory integration and the experience of scene instability, presence and cybersickness in virtual environments, Computers in Human Behavior 113 (2020) 106484.
[30] S. Palmisano, S. Summersby, R.G. Davies, J. Kim, Stereoscopic advantages for vection induced by radial, circular, and spiral optic flows, Journal of Vision 16 (2016) 7–7.
[31] R.S. Allison, A. Ash, S. Palmisano, Binocular contributions to linear vertical vection, Journal of Vision 14 (2014) 5–5.
[32] E. Nalivaiko, S.L. Davis, K.L. Blackmore, A. Vakulin, K.V. Nesbitt, Cybersickness provoked by head-mounted display affects cutaneous vascular tone, heart rate and reaction time, Physiology & behavior 151 (2015) 583–590.
[33] E. Krokos, A. Varshney, Quantifying vr cybersickness using eeg, Virtual Reality 26 (2022) 77–89.
[34] H. Oh, W. Son, Cybersickness and its severity arising from virtual reality content: A comprehensive study, Sensors 22 (2022) 1314.
[35] B.D. Lawson, P. Proietti, O. Burov, P. Sjölund, T. Rodabaugh, R. Kirollos, M. Bloch, –factors impacting cybersickness, Guidelines for Mitigating Cybersickness in Virtual Reality Systems (2022).
[36] M. Kavakli, I. Kartiko, J. Porte, N. Bigoin, Effects of digital content on motion sickness in immersive virtual environments, in: 3rd International Conference on Computer Science & Information Systems, July, 2008, pp. 23–24.
[37] L. Terenzi, P. Zaal, Rotational and translational velocity and acceleration thresholds for the onset of cybersickness in virtual reality, in: AIAA Scitech 2020 Forum, 2020, p. 0171.
[38] B. Cebeci, U. Celikcan, T.K. Capin, A comprehensive study of the affective and physiological responses induced by dynamic virtual reality environments, Computer Animation and Virtual Worlds (2019) e1893.
[39] S.A.A. Naqvi, N. Badruddin, A.S. Malik, W. Hazabbah, B. Abdullah, Does 3d produce more symptoms of visually induced motion sickness?, in: 2013 35th Annual International Conference of the IEEE Engineering in Medicine and Biology Society (EMBC), IEEE, 2013, pp. 6405–6408.
[40] M.S. Dennison, A.Z. Wisti, M. D'Zmura, Use of physiological signals to predict cybersickness, Displays 44 (2016) 42–52.
[41] Y.Y. Kim, H.J. Kim, E.N. Kim, H.D. Ko, H.T. Kim, Characteristic changes in the physiological components of cybersickness, Psychophysiology 42 (2005) 616–625.
[42] S.C. Chung, J. You, J. Kwon, B. Lee, G. Tack, J. Yi, S. Lee, Differences in psychophysiological responses due to simulator sickness sensitivity, in: World Congress on Medical Physics and Biomedical Engineering 2006, Springer, 2007, pp. 1218–1221.
[43] Y.C. Chen, J.R. Duann, S.W. Chuang, C.L. Lin, L.W. Ko, T.P. Jung, C.T. Lin, Spatial and temporal eeg dynamics of motion sickness, NeuroImage 49 (2010) 2862–2870.
[44] K.M. Jang, M. Kwon, S.G. Nam, D. Kim, H.K. Lim, Estimating objective (eeg) and subjective (ssq) cybersickness in people with susceptibility to motion sickness, Applied Ergonomics 102 (2022) 103731.
[45] M. Nürnberger, C. Klingner, O.W. Witte, S. Brodoehl, Mismatch of visual-vestibular information in virtual reality: Is motion sickness part of the brains attempt to reduce the prediction error?, Frontiers in human neuroscience (2021) 648.
[46] C. Ware, Dynamic stereo displays, in: Proceedings of the SIGCHI Conference on Human Factors in Computing Systems, CHI '95, ACM Press/Addison-Wesley Publishing Co., USA, 1995, p. 310–316. URL: https://doi.org/10.1145/223904.223944. doi:10.1145/223904.223944.
[47] C. Ware, C. Gobrecht, M. Paton, Dynamic adjustment of stereo display parameters, IEEE Transactions on Systems, Man, and Cybernetics - Part A: Systems and Humans 28 (1998) 56–65.
[48] S. Palmisano, S. Nakamura, R. Allison, B. Riecke, The stereoscopic advantage for vection persists despite reversed disparity, Attention, Perception, & Psychophysics 82 (2020).
[49] S. Palmisano, R. Davies, K. Brooks, Vection strength increases with simulated eye-separation, Attention, Perception, & Psychophysics 81 (2018).
[50] W.D. Park, S.W. Jang, Y.H. Kim, G.A. Kim, W. Son, Y.S. Kim, A study

on cyber sickness reduction by oculo-motor exercise performed immediately prior to viewing virtual reality (vr) content on head mounted display (hmd), Vibroengineering PROCEDIA 14 (2017) 260–264.
[51] S. Palmisano, L. Szalla, J. Kim, Monocular viewing protects against cybersickness produced by head movements in the oculus rift, in: 25th ACM Symposium on Virtual Reality Software and Technology, 2019, pp. 1–2.
[52] Y.J. Kim, E.C. Lee, Eeg based comparative measurement of visual fatigue caused by 2d and 3d displays, in: International Conference on Human-Computer Interaction, Springer, 2011, pp. 289–292.
[53] B. Zou, Y. Liu, M. Guo, Y. Wang, Eeg-based assessment of stereoscopic 3d visual fatigue caused by vergence-accommodation conflict, Journal of Display Technology 11 (2015) 1076–1083.
[54] Y. Zheng, X. Zhao, L. Yao, The assessment of the visual discomfort caused by vergence-accommodation conflicts based on eeg, Journal of the Society for Information Display (2019).
[55] C. Yildirim, Cybersickness during vr gaming undermines game enjoyment: A mediation model, Displays 59 (2019) 35–43.
[56] C. Yildirim, Don't make me sick: investigating the incidence of cybersickness in commercial virtual reality headsets, Virtual Reality (2019) 1–9.
[57] A. Somrak, I. Humar, M.S. Hossain, M.F. Alhamid, M.A. Hossain, J. Guna, Estimating vr sickness and user experience using different hmd technologies: An evaluation study, Future Generation Computer Systems 94 (2019) 302–316.
[58] S. Wibirama, P.I. Santosa, P. Widyarani, N. Brilianto, W. Hafidh, Physical discomfort and eye movements during arbitrary and optical flow-like motions in stereo 3d contents, Virtual Reality (2019) 1–13.
[59] E. Avan, T.K. Capin, H. Gurcay, U. Celikcan, Enhancing vr experience with rbf interpolation based dynamic tuning of stereoscopic rendering, Computers & Graphics 102 (2022) 390–401.
[60] Emotiv epoc+, `https://www.emotiv.com/epoc/`, 2022. Accessed: 2022-10-04.
[61] F. Lotte, A tutorial on eeg signal-processing techniques for mental-state recognition in brain–computer interfaces, Guide to brain-computer music interfacing (2014) 133–161.
[62] A.J. Parker, Binocular depth perception and the cerebral cortex, Nature Reviews Neuroscience 8 (2007) 379–391.
[63] D. Blackwood, W.J. Muir, Cognitive brain potentials and their application, The British Journal of Psychiatry 157 (1990) 96–101.
[64] A. Delorme, S. Makeig, Eeglab: an open source toolbox for analysis of single-trial eeg dynamics including independent component analysis, Journal of neuroscience methods 134 (2004) 9–21.
[65] I. Winkler, S. Haufe, M. Tangermann, Automatic classification of artifactual ica-components for artifact removal in eeg signals, Behavioral and Brain Functions 7 (2011) 30.
[66] R. Mahajan, B.I. Morshed, Unsupervised eye blink artifact denoising of eeg data with modified multiscale sample entropy, kurtosis, and wavelet-ica, IEEE journal of Biomedical and Health Informatics 19 (2014) 158–165.
[67] L. Pion-Tonachini, K. Kreutz-Delgado, S. Makeig, Iclabel: An automated electroencephalographic independent component classifier, dataset, and website, NeuroImage 198 (2019) 181–197.
[68] J. Kim, J. Seo, T.H. Laine, Detecting boredom from eye gaze and eeg, Biomedical Signal Processing and Control 46 (2018) 302–313.
[69] JASP Team, JASP (Version 0.11.1)[Computer software], 2019. URL: `https://jasp-stats.org/`.
[70] J. Häkkinen, F. Ohta, T. Kawai, Time course of sickness symptoms with hmd viewing of 360-degree videos, Electronic Imaging 2019 (2019) 60403–1.
[71] Y. Wang, G. Zhai, S. Chen, X. Min, Z. Gao, X. Song, Assessment of eye fatigue caused by head-mounted displays using eye-tracking, Biomedical engineering online 18 (2019) 111.
[72] C.T. Lin, S.F. Tsai, L.W. Ko, Eeg-based learning system for online motion sickness level estimation in a dynamic vehicle environment, IEEE transactions on neural networks and learning systems 24 (2013) 1689–1700.
[73] K.M.T. Pöhlmann, J. Föcker, P. Dickinson, A. Parke, L. O'Hare, The effect of motion direction and eccentricity on vection, vr sickness and head movements in virtual reality, Multisensory Research 34 (2021) 623–662.
[74] K.M.T. Pöhlmann, J. Föcker, P. Dickinson, A. Parke, L. O'Hare, The relationship between vection, cybersickness and head movements elicited by illusory motion in virtual reality, Displays 71 (2022) 102111.
[75] R. Liu, S. Cui, Y. Zhao, X. Chen, L. Yi, A.D. Hwang, Vimsnet: an effective network for visually induced motion sickness detection, Signal, Image and Video Processing (2022) 1–8.
[76] Y. Wang, J.R. Chardonnet, F. Merienne, J. Ovtcharova, Using fuzzy logic to involve individual differences for predicting cybersickness during vr navigation, in: 2021 IEEE Virtual Reality and 3D User Interfaces (VR), IEEE, 2021, pp. 373–381.
[77] H. Ved, C. Yildirim, Detecting mental workload in virtual reality using eeg spectral data: A deep learning approach, in: 2021 IEEE International Conference on Artificial Intelligence and Virtual Reality (AIVR), IEEE, 2021, pp. 173–178.